Defence Science Journal, Vol. 55, No. 1, January 2005, pp. 63-74
© 2005, DESIDOC

Synthesis of Corrosion-resistant Nanocrystalline Nickle-copper Alloy Coatings by Pulse-plating Technique

S.K. Ghosh, A.K. Grover, G.K. Dey, and A.K. Suri

Bhabha Atomic Research Centre, Mumbai–400 085

ABSTRACT

Bright and smooth nanocrystalline Monel-type *Ni-Cu* alloy gets deposited from complex citrate electrolyte by pulse electrolysis. Transmission electron microscopy studies have revealed that the deposited *Ni-Cu* alloy was nanocrystalline in nature and it comprised a two-phase (fcc+$L1_0$) mixture. The presence of twins could be seen in the nanocrystals. The *Ni-Cu* alloys prepared by pulse electrolysis were finer grained (~ 2.5-28.5 nm) than those deposited by direct current method. Nelson-Riley function has been used to calculate the lattice parameters for both the pulse current-plated and direct current-plated alloys from x-ray diffraction analysis. The microhardness values for pulse current-plated alloys were higher than for the direct current-plated alloys. The internal stresses of both the pulse current-deposited and the direct current-deposited alloys have also been measured; the values were lower for pulse current-plated alloys. Potentiodynamic polarisation studies were carried out in aerated and deaerated neutral 3.0 Wt per cent *NaCl* solution and instantaneous corrosion current density of the plated alloy was determined and compared with the Monel-400 alloy. It was found that nanocrystalline pulse current-*Ni*-35.8 Wt per cent copper alloy exhibited lower instantaneous value of corrosion current density than that of specimens with direct current method and Monel-400 alloy. The dissolution behaviour of the deposited nanocrystalline material was found to be more like general corrosion rather than localised corrosion as in the case of Monel-400 alloy.

Keywords: Monel-400 alloy, corrosion-resistant alloys, nickel-copper alloys, pulse electrolysis, nanocrystalline alloys, nanocrystals, pulse current-plating technique, corrosion current density, direct current-plating technique

1. INTRODUCTION

The nickel-copper alloy coatings had earlier been used mainly for the decorative purposes; in recent times, there has been renewed interest in the electrodeposition of *Ni-Cu* alloy coatings[1-2] and their multilayers[3-4], because of their exciting mechanical, electrical, and catalytic properties, and corrosion resistance. Especially *Ni-Cu* alloy containing about 30.0 Wt per cent copper is passive and prone to localised corrosion in seawater but shows good corrosion resistance against aerated, acidic, and alkaline media, and in many oxidising environments. The direct current electrolysis had been used extensively to obtain thick, crack-free *Ni-Cu* alloy coatings of known composition. But continuous current flow through the solution in direct current-plating bath leads to rough deposit, and sometimes it destabilises the bath, producing a decomposition product. To avoid this problem, and to get better quality coatings, pulse current-plating technique is used; pulse-plating technique is reported to decrease porosity, internal

Revised 20 April 2004

stress, impurity, and hydrogen content, increases brightness and enables a better control over the deposited composition[1].

Roos[5], *et al.* have developed the sulphate-citrate electrolyte and Chassiang[1],*et al.* have enabled *Ni-Cu* alloy to be obtained easily using pulse-plating technique. Recently, Roy[2], *et al.* and Green[6], *et al.* have studied the dissolution of nickel during pulse off-time and its effect on the composition. They have also tried to obtain stable citrate bath with very high efficiency, but it was having very low concentration of copper, so from the practical point of view, it is very difficult to operate the bath on a continuous basis. There is no reported literature which dealt with the structural characterisation of the electrodeposited *Ni-Cu* alloy coatings and their correlations with the observed mechanical properties. Studies on the electrochemical behaviour of these pulse-plated alloys are also scanty.

Considering this background, the present study comprises comparative evaluation of electrodeposited *Ni-Cu* by both direct current-plating as well as pulse current-plating techniques and using modern characterisation techniques, such as transmission electron microscopy (TEM), x-ray diffraction. The corrosion behaviour of different pulse current-plated *Ni-Cu* alloys has also been determined and the results compared with the direct current-plated *Ni-Cu* alloys and commercial Monel-400 alloy.

2. EXPERIMENTAL PROCEDURE

In the course of pulse plating of binary alloys, the applied current is cycled between a high and low value of pulse current or zero current. At high pulse current density, both the cations ($Ni^{+2} + Cu^{+2}$) of the alloy are discharged on the cathode surface. In the present experiment, a pulse current (I_p) was applied for a period of T_{on}, followed by a relaxation time (T_{off}) with no current flowing across the electrodes. The duration of the pulses was of the order of millisecond.

A complex citrate bath was used for the deposition. The bath composition was: $NiSO_4 . 7H_2O$ (0.475 M), $CuSO_4 . 5H_2O$ (0.125 M), and sodium citrate (0.20 M); the pH of the bath was 9.0 and was adjusted by ammonia solution. The citrate bath was quite stable except at temperature $\geq$ 313 K, where the citrate bath became unstable after two-to-three batches of operations. For chemical analysis of the deposits, a platinised titanium was used as substrate to dissolve the coating in nitric acid. An insoluble *Ni*-mesh was used as the anode. The electrochemical deposition was carried out at room temperature (296 $\pm$ 2K) from a quiescent solution. For corrosion studies, nanocrystalline alloy was deposited on routinely polished (up to 1 μm diamond paste) mild steel substrate and the thickness of the deposit was approx. ~15 μm calculated from the weight deposited and the compositional analysis. All the substrates were cleaned using standard alkaline solution to degrease the surface and were finally dipped in acid (10 % H_2SO_4) for 30 s prior to the deposition. A standard oscilloscope was used to measure the rectangular pulses supplied by pulse power supply. After deposition, the chemical composition of the alloy was analysed by the atomic absorption spectroscopic method.

The deposition was found to be highly adherent to the substrate. High resolution TEM (HR-TEM) revealed that the deposited nanocrystalline *Ni-Cu* alloy was dense and free from voids. Knoop hardness of the deposit (15-20 μm thick) was measured using 300 Tukon micro-indentation hardness tester. The values of microhardness were measured with a load of 50 gf. Internal stress was measured using gearless Brenner Senderoff's spiral contractometer. A Philips PW1710 diffractometer was used for x-ray diffraction studies. For TEM studies, electroformed *Ni-Cu* alloy foils were thinned by electropolishing at a cell potential of 20 V in a solution of composition 10 per cent v/v perchloric acid and 90 per cent v/v methanol cooled at 243 K. The TEM observations were carried out using a JEOL-3010 electron microscope operating at 300 kV.

The corrosion behaviour of the alloys deposited both by pulse current and direct current electrolysis and commercial Monel-400 sample was studied by potentiodynamic polarisation, both in aerated and deaerated 3.0 Wt per cent $NaCl$ solution at room temperature and at 323 K, at a scan rate of 1 mVs^{-1} in Greene-type of cell. Platinum was used as counter electrode. All potentials referred to were wrt saturated calomel electrode.

The corrosion current density (I_{corr}) was determined by Tafel extrapolation of the cathodic polarisation curves. The corroded surface was examined under optical microscope after potentiodynamic polarisation in deaerated 3.0 Wt per cent *NaCl* solution in the sweeping range –900 mV to +150 mV. The pitting potential was determined by carrying out potentiodynamic anodic polarisation at a scan rate of 0.166 mVs^{-1} in aerated condition. The anodic polarisation was continued till pitting occurred. The critical pitting potential (E_p) was measured when there was a sharp increase in the anodic current[7] ≥ 10 μAcm^{-2}.

3. RESULTS & DISCUSSION

3.1 Effect of Pulse Frequency

The pulse frequency was varied from 1 Hz to 1000 Hz by keeping peak current density, I_p (= 2000 A m^{-2}), average current density, I_a (= 200 A m^{-2}) and duty cycle, θ (= 10 %) fixed. The copper content of the deposit was largely influenced by the pulse frequency, it decreased with the increase in the pulse frequency, f (Fig. 1). Initially, the copper content of the deposit decreased appreciably

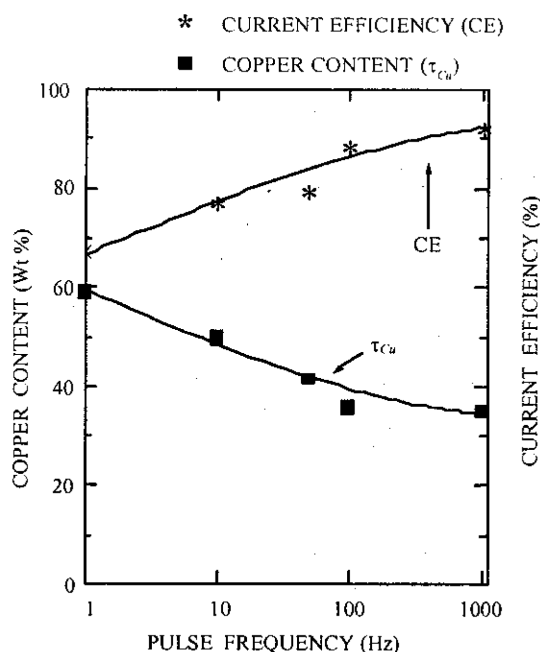

Figure 1. Effect of pulse frequency on copper content (τ_{Cu}) and the current efficiency (CE) of the alloy deposition; I_p = 2000 A m^{-2}, I_a = 200 A m^{-2}, duty cycle, θ = 10 %.

as the pulse frequency was changed from 1 Hz to 100 Hz; afterwards, it remained practically constant. The current efficiency was increased from 71.0 per cent to 83.5 per cent as the pulse frequency increased from 1 Hz to 50 Hz; the current efficiency continued to increase with the pulse frequency, attaining a value of 93.0-96.0 per cent at 1000 Hz. The coating was coherent and bright in the pulse frequency range 10 Hz to 100 Hz, but with further increase of the pulse frequency, dull, grey and rough deposits were obtained. The working pulse frequency range for obtaining good quality *Ni*-rich coating was 10-100 Hz.

The decrease in copper content with the increase in the pulse frequency could be explained in terms of corrosion and a two-step discharge model[2,8,9] during pulse-current plating. At constant duty cycle, θ (=10 %) keeping average I_a (= 200 A m^{-2}) as well as peak current density, I_p (= 2000 A m^{-2}) constant, increase in the frequency would be accomplished with the decrease in the pulse off-time as well as pulse on-time. However, copper being higher noble metal in standard emf series, nickel gets dissolved away from the deposit to solution in exchange of copper during the pulse off-time. Therefore, the overall copper concentration within the deposited alloy increases with the increase in pulse off-time (or better to say, with the decrease in the pulse frequency) because of the non-faradic displacement reaction during pulse plating. This corrosion model also suggests that the overall composition of the direct current-plated alloy would be the same as that of the pulse current-plated alloy, if the average current density remains the same. In the present study, it was also observed that the composition of the deposited alloy at higher pulse frequency approached towards that of the direct current condition; at the same average current density. On the other hand, larger pulse off-time also helps in replenishment of the Cu^{+2} ions in the (minor constituent in the electrolyte) depleted diffusion layer via various mass-transport effects, resulting in higher concentration of copper in the deposit.

The lower current efficiency at lower pulse frequency could be attributed to higher rate of hydrogen evolution. Since at high pulse on-time

(at lower pulse frequency) at fixed I_p, I_a, and θ, due to rapid discharge of the depositable ionic species, depletion in concentration wrt the bulk is being developed near the cathode surface locally. However, during galvanostatic deposition, the rate of supply of electrons onto the cathode surface is being maintained throughout the pulse on-time, therefore, to maintain the kinetic rate of discharge, H^+ ions are getting reduced, decreasing the plating current efficiency.

3.2 Effect of Average Current Density

Figure 2 shows the effect of average current density, I_a on the copper content and on the current efficiency of the electrodeposition, keeping the peak current density, I_p (= 2000 A m^{-2}); pulse frequency, f (=100 Hz), and total pulse time, T (= 10 ms) fixed. The copper content of the alloy decreased with the increase of average current density, I_a; the decrease was sharp as the current density changed from 50 A m^{-2} to 100 A m^{-2}, but with further increase in the current density, the rate of decrease was slow. The partial current for nickel deposition increases much more readily than the partial current for copper deposition[10], thus, copper content of the alloy deposit decreases with increase in the average current density. The influence on the current efficiency was not significant. The coating was of copper colour at 50 A m^{-2} but had become bright, uniform, smooth, and metallic in the range 200 Am^{-2} to 400 Am^{-2}, and at still higher current density, it was greyish, with black powdery texture.

The composition of *Ni-Cu* alloy and the current efficiency of alloy deposited under direct current condition have also been included in Fig. 2. The copper content of the alloy plated under direct current condition at 200 A m^{-2} was 30.6 Wt per cent and the corresponding current efficiency of the alloy deposition was 87.0 per cent. The current efficiency under pulsed condition at the same average current density was 92.6 per cent, indicating the higher rate of deposition, which is due to lower rate of evolution of hydrogen. The alloy plated at 2 A dm^{-2} under direct current condition was smooth, semi-bright, and metallic in texture.

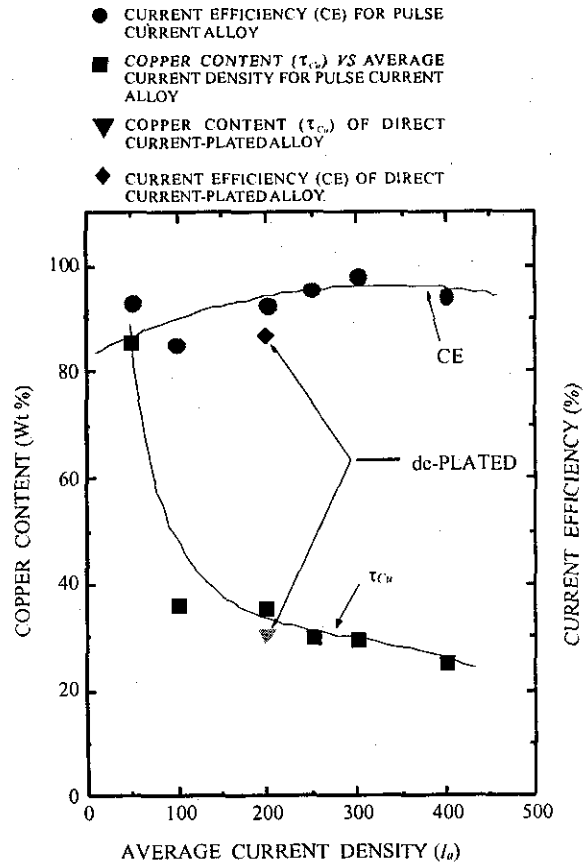

Figure 2. Effect of average current density (I_a) on copper content (τ_{Cu}) and the current efficiency (CE) of the alloy deposition: I_p = 2000 A m^{-2}, f = 100 Hz, total time, T= 10 ms. The copper content, and current efficiency of the alloy plated under direct current-plating condition at the current density 200 A m^{-2} is also shown.

3.3 X-ray Diffraction Analysis

The typical x-ray diffraction patterns (Fig. 3) of both the pulse current-plated and direct current-plated *Ni-Cu* alloy coatings reflect that in both the cases, the coating was polycrystalline and two-phase in nature, and is textured in the (111) direction. It consists of disordered fcc phase and small volume fraction of ordered $L1_0$ phase, which imparts very high hardness to the deposited alloy. The lattice parameter (a_0) of the alloy was calculated from the x-ray peak position of (111) and (222) lattice plane reflection (*hkl*) for both the direct current-plated and pulse current-plated samples. The a_{hkl} values obtained for each reflex have been plotted against the Nelson-Riley function, f_{NR} and interpolated to f_{NR} = 0, which gives the lattice parameter a_0 as

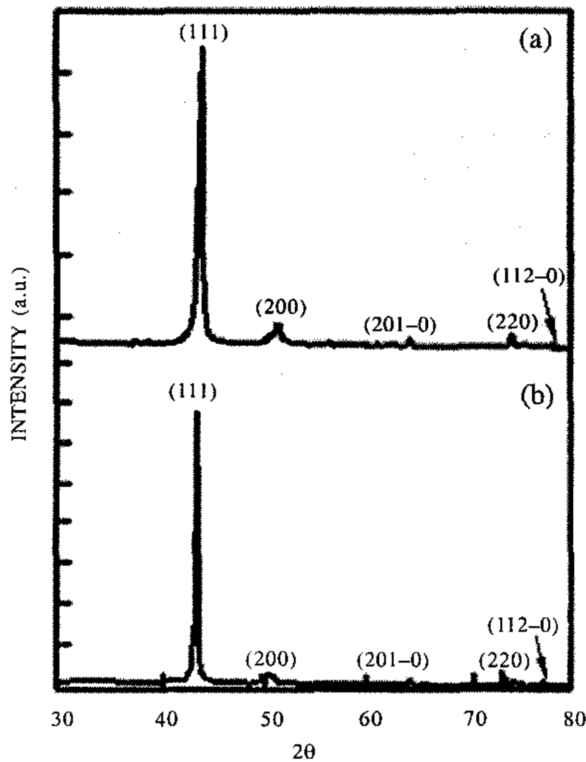

Figure 3. X-ray diffraction pattern of nanocrystalline: (a) PC-*Ni*-35.8 Wt per cent copper alloy and (b) dc-*Ni*-30.6 Wt per cent copper alloy.

mentioned in Table 1. The microstrain of the alloy was calculated by Wagner and Aqua method[11].

3.4 Surface Morphology & Microstructural Studies

The scanning electron microscopic examination revealed that smooth, silver-mirror like bright surface finish of the *Ni-Cu* alloy coating can be obtained by suitably adjusting the pulse parameters. In direct current-plated sample (I = 200 A m^{-2}), nodular structure with grain boundaries was visible [Fig. 4(a)], but at the same average current density for the pulse-plated sample (I_a = 200 A m^{-2}), the surface became smoother with no characteristic structure, mainly because of fine-grained deposit [Fig. 4(b)].

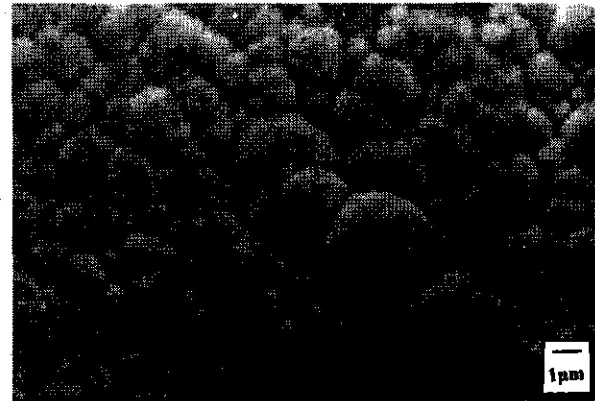

(a)

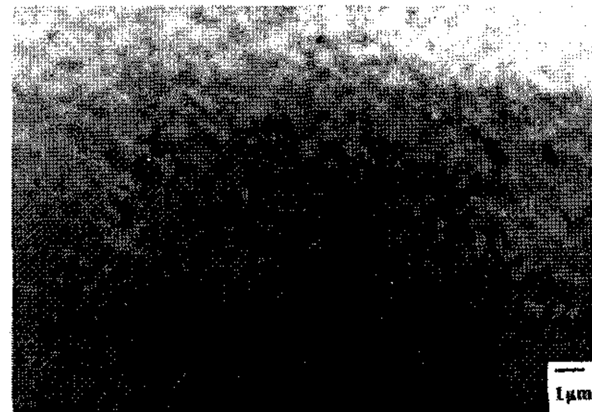

(b)

Figure 4. Scanning electron microscope image of the surface topography of electrodeposited alloys: (a) dc-*Ni*-30.6 Wt per cent copper deposited at current density 200 A m^{-2}, pH=9.0 (b) PC-*Ni*-35.8 Wt per cent copper deposited at I_p = 2000 A m^{-2}, I_a = 200 A m^{-2}, f = 100 Hz, duty cycle (θ) = 10 per cent, pH= 9.0.

Table 1. Residual stress, microhardness, microstrain, average crystallite and lattice parameter of pulse current-plated, direct current-plated alloys and Monel-400

Sample	Residual stress at 5 μm (MPa)	Micro-hardness ($KHN_{50\,gf}$)	Microstrain $\langle\varepsilon^2\rangle^{1/2}\times10^3$	Crystallite size (nm) TEM (Avg)	$^*I_{Corr}$ (A m^{-2})	Lattice parameter (nm)
PC-*Ni*-27.4 Wt % *Cu*	60.34	482	3.5166	7.8	-	-
dc *Ni*-30.6 Wt % *Cu*	81.6	400	3.7639	27.8	0.06	0.35503
PC *Ni*- 35.8 Wt % *Cu*	42.5	452	3.6843	12.7	0.015	0.35605
Monel-400 31.5 Wt % *Cu*	-	260	-	~15,000	0.022	-

* Deaerated 3.0 Wt per cent *NaCl* solution, 323 K

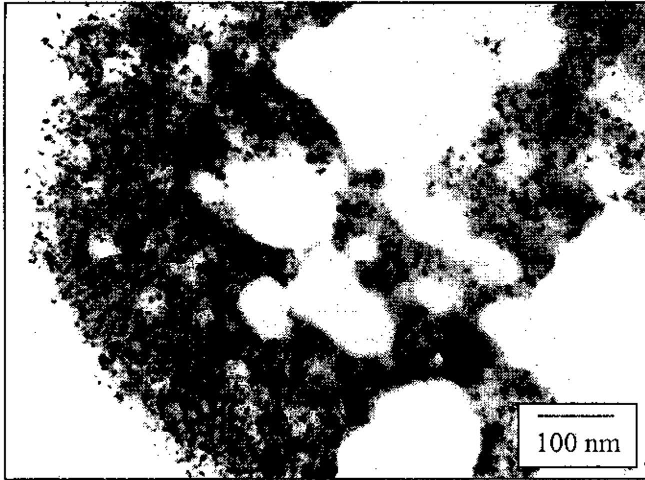

(a)

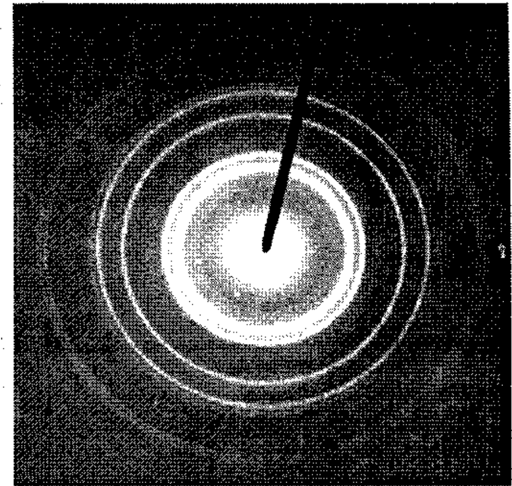

(b)

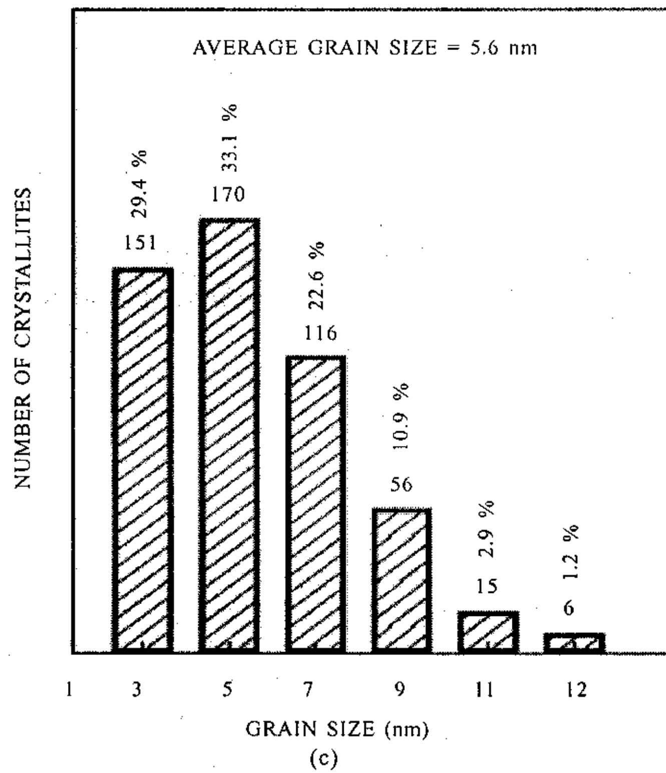

(c)

Figure 5. (a) Transmission electron microscopic bright field image of the pulse current-plated *Ni*-26.0 Wt per cent copper alloy deposited at I_p = 2000 A m^{-2}, I_a = 400 A m^{-2}, f = 50 Hz, duty cycle (θ) = 20 per cent, p*H* = 9.0, at room temperature; (b) selected area electron diffraction (SAED) pattern of the same specimen, and (c) crystallite size distribution of the same specimen.

The pulse plating method thus has a distinct advantage in that a very large peak current density(I_p = 4000 A m^{-2}), can be applied and still a good surface finish is achieved, whereas in direct current-plating, the current density must not exceed 300-400 A m^{-2}, otherwise powdery deposits are formed. Because of high energy involved in pulse plating[10], generation of fresh nucleation centres during the pulse time is more, which facilitate the production of finer-grained crystallites.

The transmission electron microscopic examination of *Ni*-35.8 Wt per cent copper sample produced at

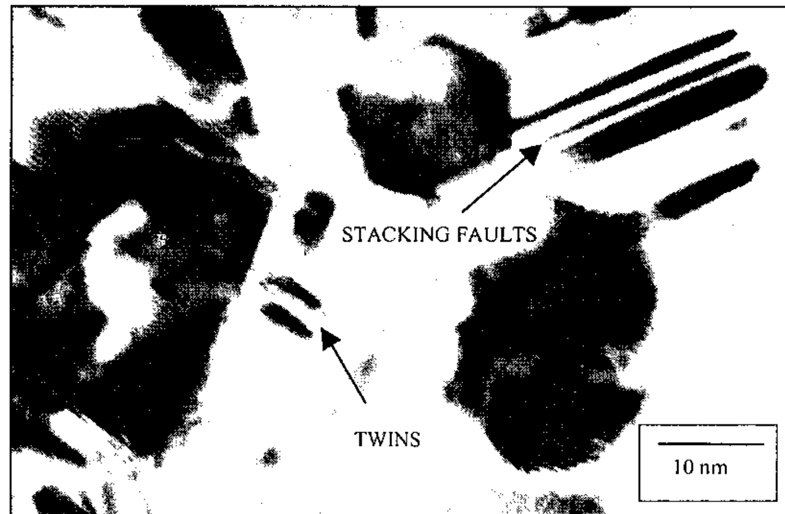

Figure 6. High resolution transmission electron microscopic examination of the PC-*Ni*-27.4 Wt per cent copper alloys plated under pulse current-plating condition: I_p = 2000 A m^{-2}, I_a = 400 A m^{-2}, f = 100 Hz, and duty cycle (θ) = 20 per cent, showing twins, stacking fault, and faceted morphology.

pulse frequency 100 Hz, peak current density 2000 A m^{-2}, the average current density 200 A m^{-2} showed nanocrystalline structure and the measurement of crystallite size showed that crystallites were in the size range 2.5 nm to 28.5 nm, the average being 12.7 nm. When the average current density was increased to 400 A m^{-2}, at pulse frequency 50 Hz, peak current density 2000 A m^{-2}, there was refinement in the crystallite size [Fig. 5(a)]; it ranged between 0.6 nm to 12.6 nm, the average size being 5.6 nm. Figure 5(b) is the corresponding selected area electron diffraction (SAED) pattern of the alloy, which indicates the presence of ultrafine structure. The crystallite size distribution is also shown in Fig. 5(b).

The TEM examination of the specimens produced by application of direct current at the current density of 200 A m^{-2} showed a relatively larger grain size in the range 10 nm to 74 nm, the average being 27.8 nm, as mentioned in Table 1. In addition, it was also possible to observe the morphology of the nanograins. It could be seen that the grains, instead of being spherical, have a faceted morphology (Fig. 6), which is indicative of crystallographically unisotropic growth. The dislocations are rarely seen in nano particles, and this study was no exceptions in this regard. Besides twins, it was possible to see features which resembled stacking faults in the grains (Fig. 6).

3.5 Mechanical Properties

The hardness of a material depends on the crystallite size. Smaller the crystallite size, higher is the compactness and lesser is the porosity within the alloy. As the deposited alloy is nanocrystalline in nature (crystallite size ~ 2.5 nm–28.5 nm), the hardness is expected to be higher than the direct current-plated samples, where the crystallite sizes are larger as shown in Table 1.

The internal stress of the deposited alloy is tensile in nature. In Table 1, the tensile stress value has been given at a thickness of 5 μm. Tensile stress is higher for the direct current-plated sample than the pulse current-plated sample, as deposited under similar conditions.

3.6 Corrosion Studies

The results on the potentiodynamic polarisation experiments at room temperature in 3.0 Wt per cent *NaCl* solution (Fig. 7) without purging argon or nitrogen indicated that synthesised nanophase pulse current-plated *Ni-Cu* alloy was better than the synthesised direct current-plated alloys wrt its open-circuit-potential and corrosion current density, I_{corr}. Both the open circuit potential –174 mV and the instantaneous corrosion current density, I_{corr} = 9.58 × 10^{-2} A m^{-2} values for pulse current-

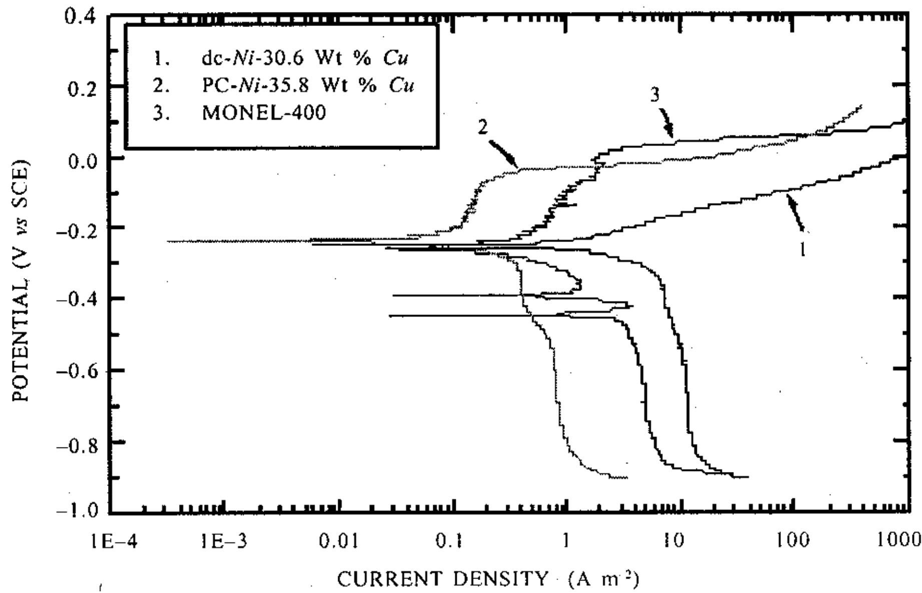

Figure 7. Potentiodynamic polarisation plots of PC-35.8 Wt per cent copper, dc-30.6 Wt per cent copper and Monel-400 alloys in aerated 3.0 Wt per cent *NaCl* solution at 298 K and p*H* = 7.0.

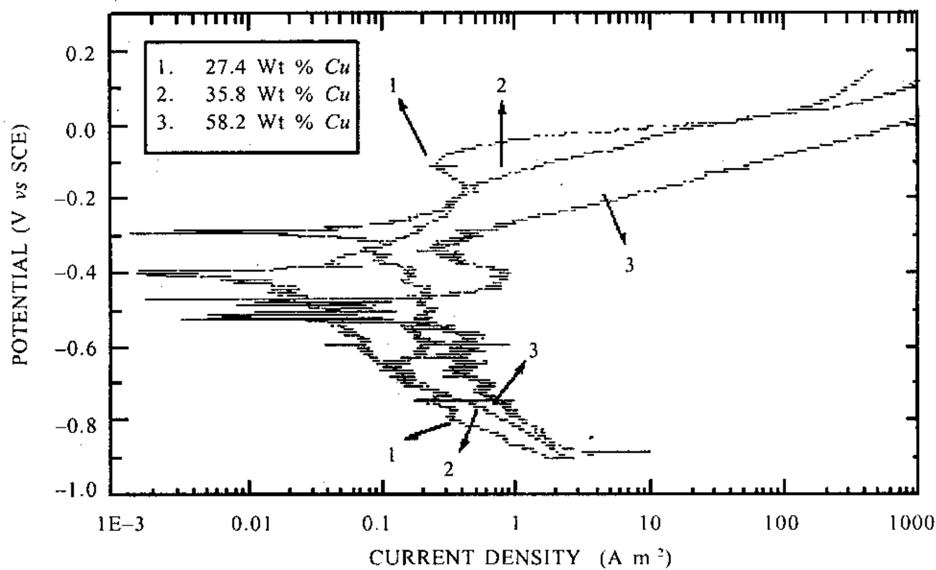

Figure 8. Potentiodynamic polarisation plots of PC-plated *Ni-Cu* alloys in deaerated 3.0 Wt per cent *NaCl* solution at 323 K and p*H* = 7.0.

Ni-35.8 Wt per cent copper alloy were better than Monel-400, open circuit potential –225 mV, I_{corr} = 20.48 ×10^{-2} A m^{-2}, and for direct current-*Ni*-30.6 Wt per cent copper are –180 mV, I_{corr} = 40.29 × 10^{-2} A m^{-2} respectively. Although the passive region for pulse current-*Ni*-35.8 Wt per cent copper alloy was smaller than for the Monel-400, the anodic current density corresponding to its plateau region was lower than the latter. Figure 8 presents the cathodic and the anodic potentiodynamic polarisation of pulse-plated *Ni-Cu* alloy (coating thickness 15-20 μm) at 323 K in deaerated 3.0 Wt per cent *NaCl* solution. In deaerated condition, pulse current-*Ni*-35.8 Wt per cent copper showed more or less active behaviour compared to the other two pulse current-plated alloys, which exhibited active-passive-transpassive

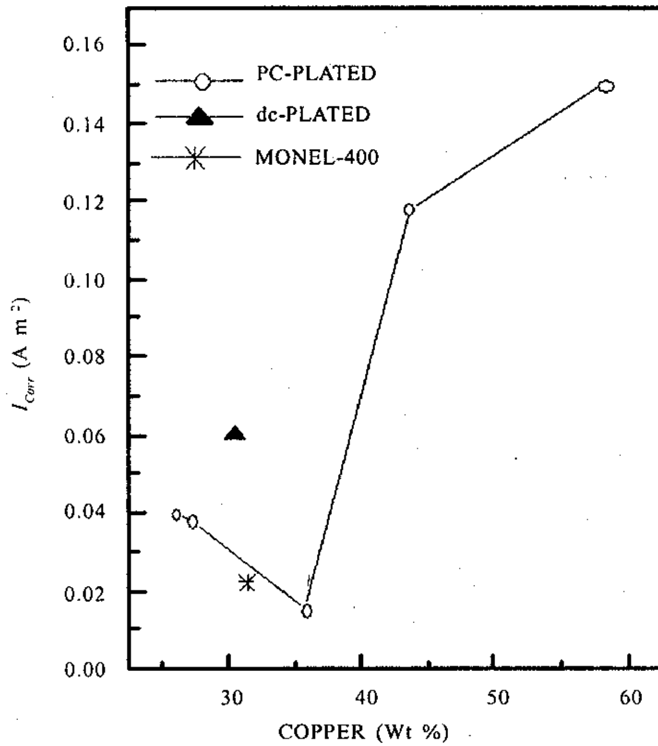

Figure 9. Effect of copper content on the corrosion rate of *Ni-Cu* alloys in 3.0 Wt per cent *NaCl* solution at 323 K and p*H* = 7.0.

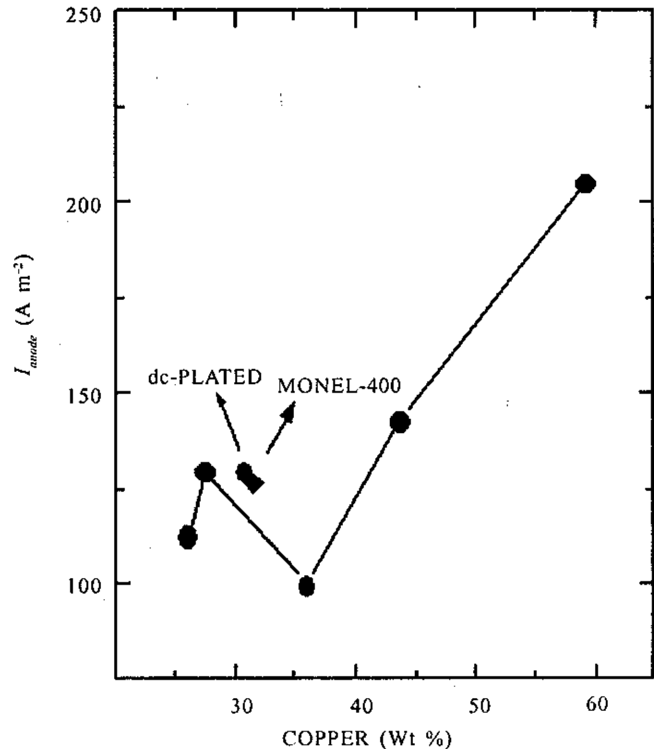

Figure 10. Effect of copper content on the anodic current density (I_{anode}) at –50 mV in deaerated 3.0 Wt per cent *NaCl* solution at 298 K and p*H* = 7.0.

behaviour. However, Fig. 9 shows that pulse current-*Ni*-35.8 Wt per cent copper alloy has the lowest corrosion rate and the calculated corrosion current density increased rapidly with 58.2 Wt per cent copper content of the pulse current-plated alloy. The behaviour of direct current-plated *Ni*-30.6 Wt per cent copper alloy is intermediate between these two pulse current-plated alloys; I_{corr} of pulse current-plated *Ni*-35.8 Wt per cent copper alloy was about one-fourth (0.015 A m^{-2}) as that for direct current-plated *Ni*-30.6 Wt per cent copper alloy (0.06 A m^{-2}). The anodic current density (I_{anode}) measured in deaerated 3.0 Wt per cent *NaCl* solution at 298 K at an anodic potential of –50 mV (Fig. 10) showed the lowest value for *Ni*-35.8 Wt per cent copper alloy.

The surface morphology of pulse current-*Ni*-35.8 Wt per cent copper and Monel-400 alloys was examined following polarisation from –900 mV (SCE) to +150 mV (SCE) at a sweep rate of 0.33 mVs^{-1}. The optical microscopy of the corroded surface of the specimens (Fig. 11) showed numerous shallow, small pits visible on the corroded nanoalloy's surface with homogeneous corrosion rather than few large, well-defined deep pits which appear on the coarser grained (Monel-400) material. It indicates that conventional materials are more susceptible to pitting corrosion than the nanoalloys.

The respective pitting potential (E_p) values as determined from the anodic potentiodynamic experiments for the Monel-400 and nanocrystalline-*Ni*-35.8 Wt per cent copper were – 44 mV and –113 mV. It was observed from the potentiostatic polarisation behaviour that there was no specific passive region for nanocrystalline-*Ni*-35.8 Wt per cent copper, however, Monel-400 showed distinct passive region. Therefore, in case of nanocrystalline-*Ni*-35.8 Wt per cent copper, the corrosion is more like a general corrosion rather than pitting corrosion. In the case of Monel-400, the rate of increase in current with potential sweep is very sharp beyond the pit initiation potential because of pit propagation compared to nc-*Ni*-35.8 Wt per cent copper. The pitting potentials for curves 2 and 3 in Fig. 7 [curve 2 (PC-*Ni*-35.8 Wt % *Cu* and curve 3

(a)

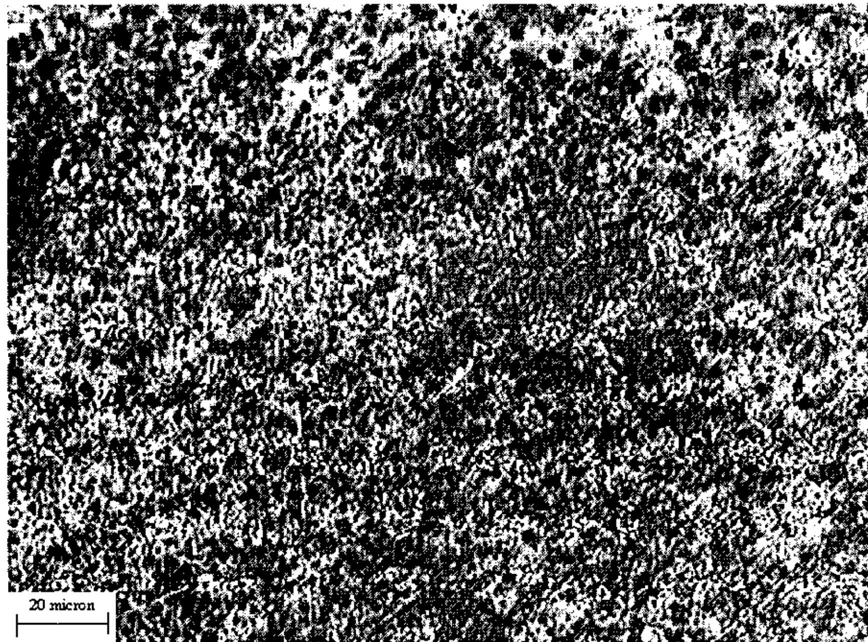

(b)

Figure 11. (a) Optical micrograph of Monel-400 and (b) PC-*Ni*-35.8 Wt per cent copper alloy after electrochemical study in the range – 900 mV to +150 mV (SCE) in deaerated 3.0 Wt per cent *NaCl* solution at room temperature and p*H* = 7.0.

(Monel-400)] are quite close to each other. Both the curves 2 and 3 indicate sharp rise in anodic current density from the pitting potential region. Both the curves 2 and 3 are similar to each other except for a decade lower value of current density in the plateau region of curve 2 in relation to that of curve 3. Therefore, material of curve 2 (pulse current plated-35.8 Wt per cent copper) can attain

passive behaviour much more quickly than the material of curve 3 (Monel-400). Thus, in respect of attaining quicker passivation, PC-35.8 Wt per cent copper was superior to Monel-400, as analysed from the above curves.

The corrosion studies highlight the superior passivation characteristics of pulse current-plated *Ni*-35.8 Wt per cent copper alloy in both aerated and deaerated conditions. The grain boundaries and other defects in nanomaterials have been identified to provide likely sites for preferential attack when the materials are exposed to a corrosive environment. In this case, the nature of high intercrystalline surface fraction or defect density in nanocrystalline materials provides a more beneficial anode/cathode surface ratio (grain boundary region acts as the anode and grain body acts as the cathode) against localised corrosion. In the present study, the pulse-plated nanocrystalline *Ni-Cu* alloy deposited under certain conditions [f = 100 Hz, I_p =2000 A m^{-2}, I_a= 200 A m^{-2}, duty cycle (θ) = 10 %] has shown superior passivation behaviour, that may lead to better corrosion-resistant behaviour because the alloy was coherent, compact, and free from the defects like porosity or voids, was seen from HR-TEM.

4. CONCLUSIONS

The smooth, coherent, bright, and nanocrystalline *Ni-Cu* alloys (copper content 26-36 Wt %) have been obtained by operating the bath at room temperature and using the pulse parameters: frequency 50-100 Hz, peak current density 2000-4000 A m^{-2}, and duty cycle 10 per cent. Internal stress values for pulse current-plated alloy are seen to be lower than the direct current-plated alloys under similar conditions. The TEM studies revealed that deposited alloys are dense and free from porosity. The study indicates that the corrosion resistance in 3 Wt per cent *NaCl* at 298 K and 323 K of the pulse-plated alloy is composition-dependent, and that overall corrosion resistance of pulse current *Ni*-35.8 Wt per cent copper is superior to direct current-plated alloy.

ACKNOWLEDGEMENT

The authors are thankful to Dr S. Banerjee, Director, Bhabha Atomic Research Centre (BARC), Mumbai, for his encouragement during the course of this study.

REFERENCES

1. Cherkaoui, M.; Chassaing, E. & VU Quang, K. *Surface Coating Technol.*, 1988, **34**, 243-52.
2. Roy, S.; Matlosz, M. & Landolt, D. *J. Electroche Soc.*, 1994, **141**, 1509-517.
3. Lashmore, D.S. & Dariel, M.P. *J. Electrochem. Soc.*, 1998, **135**, 1218-221.
4. Bird, K.D. & Schlesinger, M. *J. Electrochem. Soc.*, 1995, **142**, 165L-166L.
5. Roos, J.R.; Celis, J.P.; Buelens, C. & Goris, D. *Proc. Metall.*, 1984, **3**, 177-81.
6. Green, T.A.; Russel, A.E. & Roy, S. *J. Electrochem. Soc.*, 1998, **145**, 875-83.
7. Dayal, R.K.; Parvathavarthini, N. & Gnanamoorthy, J.B. *Corrosion*, 1980, **36**, 433-36.
8. Chassaing, E.; VU Quang, K. & Wiart, R. *J. Appl. Electrochem.*, 1987, **17**, 1267-76.
9. Ghosh, S.K.; Grover, A.K.; Dey, G.K. & Totlani, M.K. *Surface Coating Technol.*, 2000, **126**, 45-63.
10. Tannenberger, H. & Schnidler, K. *In* Proceedings of the 3rd International Pulse Plating Symposium, Washington, 28-29 October 1986, American Electroplaters and Surface Finishers Society, Orlando, FL., 1986.
11. Wagner N.J. & Aqua, E. *Adv. X-ray Anal.*, 1963, **7**, 46.

Contributors

Mr S.K. Ghosh obtained his MSc (Chemistry) in 1995 from the Burdwan University. He is working as the Scientific Officer in the Materials Processing Div of the Bhabha Atomic Research Centre (BARC), Mumbai. His research interest includes: Electrodeposition of nanocrystalline alloys and nanolayered materials from aqueous solution. He has 10 research papers to his credit.

Mr A.K. Grover is the Head, Materials Processing Div, BARC, Mumbai. He has over 36 years of R&D experience in surface engineering, in particular plating technology, electrochemical oxidation, laser surface alloying, vapour deposition, and quality evaluation of coated components. Currently, his research areas include: Electrosynthesis of nanocrystalline metals and alloys, compositionally-modulated multilayers, diffussion bonding of dissimilar materials, ceramic-to-metal seals, and development of neutron sensors. He has about 75 scientific publications to his credit.

Dr G.K. Dey obtained his PhD (Metallurgical Engg). Presently he is working as Senior Scientist in the Materials Processing Div of BARC, Mumbai. He is the recipient of two national awards. His areas of research include: Phase transformation, rapid solidification, electron microscopy and defect characterisation, and high resolution electron microscopy. He has more than 150 scientific publications to his credit.

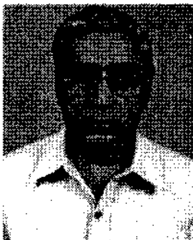

Dr A.K. Suri obtained his PhD (Metallurgical Engg). Presently, he is Assoc Director, Materials Group (P) of BARC, Mumbai. His areas of specialisation include: Chemical metallurgy, vapour deposition, and advanced processing techniques. He is the recipient of two national awards and has over 130 research papers to his credit.